

**Article type: Communication****Carrier Density Control of the SrTiO<sub>3</sub> (001) surface 2DEG studied by ARPES**

*Siobhan McKeown Walker, Flavio Yair Bruno\*, Zhiming Wang, Alberto de la Torre, Sara Riccò, Anna Tamai, Timur Kim, Moritz Hoesch, Ming Shi, Mohammad Saeed Bahramy, Phil King and Felix Baumberger*

S. McKeown Walker, Dr. F. Y. Bruno, A. de la Torre, S. Ricco, Dr. A. Tamai, Prof. F. Baumberger

Department of Quantum Matter Physics, University of Geneva, 24 Quai Ernest-Ansermet, 1211 Geneva, Switzerland

E-mail: [flavio.bruno@unige.ch](mailto:flavio.bruno@unige.ch)

Dr. Z. Wang, Dr. M. Shi, Prof. F. Baumberger

Swiss Light Source, Paul Scherrer Institute, 5232 Villigen, Switzerland

Dr. T.K. Kim, Dr. M. Hoesch

Diamond Light Source, Harwell campus, Didcot OX11 0DE, United Kingdom

Dr. Mohammad Saeed Bahramy

Quantum-Phase Electronics Center, Department of Applied Physics, University of Tokyo, 113-8656 Tokyo, Japan

RIKEN Center for Emergent Matter Science, 351-0198 Wako, Japan

Dr. P.D.C. King, Prof. F. Baumberger

School of Physics and Astronomy, University of St Andrews, KY16 9SS St Andrews, United Kingdom

Keywords: strontium titanate, angle resolved photoemission spectroscopy, two-dimensional electron gas, oxygen vacancies

Combining the tunability of semiconductor heterostructures with the rich properties of correlated electron systems is a central goal in materials science. The two-dimensional electron gas (2DEG) observed at the LaAlO<sub>3</sub>/SrTiO<sub>3</sub> (LAO/STO) interface<sup>[1]</sup> emerged as a particularly promising model system in this regard since it combines high mobility with properties such as gate-tunable superconductivity that cannot be realized in conventional semiconductor heterostructures or bulk correlated electron systems.<sup>[2-5]</sup> The interface 2DEG resides solely in STO and can be stabilized in different ways. These include interfacing STO with other crystalline insulating materials such as spinel Al<sub>2</sub>O<sub>3</sub> or perovskite GdTiO<sub>3</sub>,<sup>[6,7]</sup> deposition of amorphous overlayers,<sup>[Y. Chen et al, Nano Lett. 2011, 11, 3774. 8,9]</sup> and electrolyte gating.<sup>[10]</sup> A similar 2DEG has also been observed on the bare surface of STO following irradiation with

UV light.<sup>[11–13]</sup> Irrespective of the method by which the 2DEG is created, the electronic properties of the system are governed by carriers doped into the titanium  $3d$   $t_{2g}$  bands of STO close to the interface or surface.

Control of the 2DEG density has been achieved at the LAO/STO interface by electrostatic gating and by growing samples at different temperatures.<sup>[3,14]</sup> Subsequent electronic transport experiments have established the thermodynamic phase diagram of the 2DEG as a function of carrier density and provided evidence for a complex electronic structure with multiple orbitally polarized subbands,<sup>[3,15,16]</sup> qualitatively consistent with first-principles electronic structure calculations.<sup>[17]</sup> While there is strong indirect evidence for this picture,<sup>[18]</sup> direct measurements of the 2DEG band structure proved difficult. Quantum oscillation measurements at the LAO/STO interface were only successful in the low carrier density regime and are intrinsically restricted to the Fermi energy.<sup>[19–21]</sup> Angle-resolved photoemission (ARPES) experiments can provide direct momentum space resolution over the entire occupied bandwidth. However, ARPES experiments on buried interfaces require high excitation energies limiting the resolution and sensitivity of the measurements. Consequently, to date only a small subset of the predicted ladder of quantum well states could be resolved on the LAO/STO interface.<sup>[22,23]</sup> A clearer picture of the 2DEG electronic structure can be obtained from ARPES experiments on the bare surface of STO.<sup>[11,24,25]</sup> However, these experiments have so far been restricted to a single carrier density largely because the mechanism by which the 2DEG develops in the bare STO(001) surface under UV-light irradiation remained unclear.

Here we study this mechanism and show that we can create and fully deplete the 2DEG by alternate in-situ exposure of the surface to light and small doses of oxygen. This demonstrates that the 2DEG is an electron accumulation layer screening positively charged oxygen vacancy (OV) defects that are created in the surface by irradiating the sample with photons of appropriate energy. We establish that OVs are created via Ti  $3p$  core-hole Auger

decay. This channel is only active when photons of  $h\nu > \sim 38$  eV are used enabling us to study the electronic structure of the 2DEG by ARPES at intermediate carrier densities by employing either photons below this threshold energy, or by simultaneous irradiation and oxygen exposure.

All experiments shown in the following have been performed with lightly La-doped STO. This results in a residual bulk conductivity that facilitates photoemission experiments but has no measurable influence on the 2DEG electronic structure.<sup>[25]</sup> Figure 1a shows the electronic structure of a 2DEG with saturated bandwidth at the (001) surface of STO measured with a photon energy of 52 eV at a temperature of 10 K. Consistent with earlier experimental studies we find that the 2DEG bandwidth develops gradually under the light and eventually saturates near 250 meV. The observation of multiple orbitally polarized subbands has been interpreted as a consequence of quantum confinement due to band bending near the surface.<sup>[11,24]</sup> This picture is confirmed by the tight-binding supercell calculations following Reference <sup>[25]</sup> shown in Figure 1b, which reproduce the three light subbands (grey, green and blue lines) and the heavy subband (orange line) that are resolved by the ARPES measurement. The three light subbands have predominately  $xy$ -orbital character and form three concentric circular Fermi surface (FS) sheets. The heavy subband belongs to a pair with primarily  $xz/yz$ -orbital character forming two elliptical Fermi surface sheets with their long axes oriented along  $k_y$  and  $k_x$ , respectively.<sup>[25]</sup> To estimate the carrier density of the 2DEG we count the two dimensional Luttinger volume  $n_{2D}$  of the first light subband and the two equivalent heavy subbands. This criteria gives  $n_{2D} = 1.9 \times 10^{14} \text{ cm}^{-2}$  for Figure 1a and will be adopted in the remainder of the manuscript. We note that  $n_{2D}$  determined in this way excludes contributions from any small FS sheets of low bandwidth that are not resolved in some of our experiments and thus underestimates the carrier density. From a comparison to self-consistent tight-binding supercell calculations,<sup>[25]</sup> we estimate that  $n_{2D}$  represents approximately 70 % of the total sheet carrier density  $n_{2D\text{-total}}$  (see Supporting Information Figure S1a).

To establish that oxygen vacancies lie at the origin of the STO(001) surface 2DEG we performed a three step experiment as shown in Figures 2a-2c. Firstly we irradiate the surface with photons of 52 eV, in order to obtain the fully developed 2DEG shown in Figure 2a.<sup>[11]</sup> Secondly, we stop the photon flux and expose the surface to 0.5 Langmuir of O<sub>2</sub>. This fully depletes the 2DEG, as is evident from Figure 2b. Finally, we irradiated the sample for a second time with 52 eV photons and observe, as shown in Figure 2c, that the 2DEG has redeveloped. The entirety of the experiment was performed at 10K without moving the sample or photon beam and all data in Figure 2 were measured with 28 eV photons. This experiment confirms that the 2DEG is a quantum confined accumulation layer of electrons at the surface of STO that screens positive charge resulting from light induced defects; that the 2DEG is depleted by exposure to oxygen identifies these defects as light induced oxygen vacancies.

Figures 2d to 2f show angle-integrated valence band spectra corresponding to Figures 2a to 2c respectively. The valence band leading edge midpoint (VB LEM) is indicated by a cross in each spectrum, and its position with respect to the Fermi level ( $E_F$ ) is summarized in Figure 2g together with the 2DEG total bandwidth. The clear downward shift of the valence band on irradiated samples indicates a downward bending of the conduction band at the surface. The simultaneous observation of spectral weight at the Fermi level demonstrates that the 2DEG originates from band bending in SrTiO<sub>3</sub>, as is the case in interface 2DEGs. We note, however, that the shift of the VB LEM is only a qualitative measure of the surface band bending, since it represents an average of the local potential over a few unit cells rather than the exact potential at the surface. In the remainder of the manuscript we show that doped carriers fill Ti derived 3*d* bands, we discuss the main mechanism for the creation of oxygen vacancies at the surface and finally illustrate how this knowledge can be used in order to stabilize different carrier densities in the 2DEG.

In Figure 3a and 3b we present x-ray photoemission spectroscopy (XPS) measurements of the STO core levels O 1s and Ti 2p respectively, taken at a single position on the sample surface and with photon energy  $h\nu = 650$  eV. The XPS measurements are from a pristine as-cleaved surface (grey), after sufficient irradiation with 52 eV light to saturate the 2DEG bandwidth (green), and following oxygen exposure where the 2DEG is fully depleted again (blue). From Figure 3a we determine that the integrated intensity of the O1s peak is reduced to approximately 90% of the original value after UV irradiation and largely recovers after exposure to 0.4 L of O<sub>2</sub> ( $2.6 \cdot 10^{-9}$  mbar oxygen partial pressure for 200 s). Together these observations directly confirm the existence of OV<sub>s</sub> at the irradiated surface. Moreover, they suggest a remarkable reactivity of vacancies for the dissociation of molecular oxygen offering a possible new route to enhancing the catalytic activity of SrTiO<sub>3</sub>. That such a low dose of oxygen is sufficient to fully quench the OV<sub>s</sub> further indicates that they lie in the top few unit cells of the surface, which is plausible given the low temperature of our experiment where vacancy diffusion is negligible. Therefore, to estimate the number of OV per 2D unit cell we assume that they are located either in the topmost TiO<sub>2</sub> layer or equally distributed over the top TiO<sub>2</sub> and SrO layers. Both of these configurations are found to have a low formation energy in a recent density functional theory study and are stable at low temperature.<sup>[26]</sup> Accounting for the exponential attenuation of the photoelectron signal from subsurface layers using an inelastic mean free path of 5.5 Å, these models correspond to OV densities of  $\sim 0.53$  and  $\sim 0.62$  per 2D unit cell on a surface that we measure by ARPES to have  $n_{2D\text{-total}} \approx 0.38$  per 2D unit cell. This shows that a substantial fraction of the nominally two excess electrons per OV remain localized on the vacancy and do not contribute to the itinerant carrier density, consistent with recent theoretical studies.<sup>[26–28]</sup>

The mixed character of OV<sub>s</sub> is also reflected in the Ti 2p XPS spectra. On surfaces supporting a saturated 2DEG (green spectrum in Fig. 3b), we find a clear transfer of spectral weight towards a shoulder on the low binding energy side that can be attributed to Ti<sup>3+</sup> ions

and is also observed at the interface of both crystalline and amorphous LAO layers with STO. [Y. Chen et al, Nano Lett. 2011, 11, 3774, Y. Chen et al Adv. Mat. 2014, 26, 1462, 29,30] Fitting the XPS spectrum with four Lorentzians representing the spin-orbit split  $Ti^{3+}$  (shaded orange) and  $Ti^{4+}$  (shaded blue) peaks, as shown in Figure 3c, we find a ratio of  $Ti^{3+}/Ti^{4+}$  sites of  $\sim 20\%$ , averaged over the probing depth. In order to compare this ratio to the  $Ti^{3+}$  signal expected from the itinerant  $t_{2g}$  carriers in the 2DEG, one needs to model their depth distribution. Assuming a charge density profile as obtained from the tight-binding supercell calculations for a saturated 2DEG with  $n_{2D-total} \approx 0.4$  (see Supporting Information Figure S1b), we estimate that  $\approx 40\%$  of the  $Ti^{3+}$  signal arises from itinerant carriers in the Ti  $t_{2g}$  shell. The full experimental  $Ti^{3+}$  signal can only be reproduced with solely itinerant carriers by assuming an unphysically narrow charge distribution, where almost all carriers are localized on the topmost  $TiO_2$  layer. This leads us to conclude that  $Ti^{3+}$  sites corresponding to electrons localized on or near OVs are present in the system in addition to the  $Ti^{3+}$  sites resulting from the itinerant carriers that form the 2DEG. This is consistent with the findings from our  $O1s$  XPS data and might arise from correlation effects or the preferential occupation of localized Ti  $e_g$  states in sub-surface vacancies as discussed in recent theoretical studies.<sup>[26,27,31]</sup>

In Figure 4 we show the evolution of the valence band leading edge midpoint as a function of irradiation time measured at two different photon energies: 52 eV (solid symbols) and 26 eV (open symbols). The total shift is a qualitative measure of the direction and relative magnitude of the band bending as discussed previously (see Figure 2d-g). The VB LEM shifts away from the Fermi level as the surface is irradiated which indicates a downward band bending. This shift is small for  $\approx 2400$  seconds irradiation with 26 eV light (open circles) leading to a 2DEG bandwidth  $< 50$  meV. A saturated 2DEG with  $\approx 250$  meV bandwidth is only obtained after further exposure of the same area for comparable time with 52 eV photons, which results in a large shift of the VB LEM. It is clear from these experiments that the rate at which the VB LEM shifts, and accordingly the rate of oxygen vacancy creation, depends on

the photon energy with which the surface is irradiated. This is consistent with the observation of a threshold energy for oxygen vacancy creation by stimulated  $O^+$  desorption in maximal valence oxides first described by Knotek and Feibelman for  $TiO_2$ <sup>[32]</sup>. In this model, the incident photon creates a Ti  $3p$  core hole which is subsequently filled with electrons from neighboring O  $2p$  orbitals via an inter-atomic Auger process<sup>[33,34]</sup>. Simple Auger events remove only two electrons from the  $O^{2-}$  ion, but in some cases after a double Auger process three electrons can be removed resulting in  $O^+$ . The Coulomb repulsion from the surrounding  $Ti^{4+}$  in the lattice favors desorption of the ionized oxygen atoms thus creating oxygen vacancies. The photon energy necessary to create a Ti  $3p$  core hole in STO is  $\sim 38$  eV, explaining the much more efficient creation of oxygen vacancies when the surface is irradiated using photon energies above this threshold.

Understanding the mechanism by which the 2DEG develops allows unprecedented control of the carrier densities accessible to ARPES experiments, presenting a new opportunity to trace the evolution of the electronic structure. It is possible to proceed in at least two different ways. Firstly, we can lower the carrier density of a fully developed 2DEG by exposing the surface to low  $O_2$  doses and subsequently probe the band structure with photon energies below the Ti  $3p$  threshold. Alternatively, ARPES experiments can be performed at photon energies above this threshold but in the presence of a low  $O_2$  background pressure. The first approach is illustrated in Figure 5a and 5b where the band dispersion is studied with a photon energy of 28 eV after exposing the surface to 0.1 and 0.2 Langmuir  $O_2$  respectively. We are able to obtain high quality data of these intermediate density states because at this photon energy the carrier density barely varies in the timescale of the experiment. The second alternative is illustrated in Figure 5c and 5d where the dispersion plots were taken with a photon energy of 52 eV and at an  $O_2$  partial pressure of  $6.5 \times 10^{-10}$  and  $1.3 \times 10^{-9}$  mbar of  $O_2$  respectively. The oxygen vacancies created by the UV light are filled

with increased efficiency at higher O<sub>2</sub> partial pressure and the resulting dynamic equilibrium stabilizes different 2DEG carrier densities as has been shown for anatase TiO<sub>2</sub>.<sup>[35]</sup>

Using both methods and collecting data from different samples we have investigated the evolution of the 2DEG subband bandwidth as a function of the carrier density. The results are summarized in Figure 5e where we plot the energies of the first three light subbands and the first heavy subband shown schematically in the inset of Figure 1b. From the good agreement with single parameter linear fits we conclude that all subband energies are approximately proportional to the carrier density. This behavior is a hallmark of confinement in an asymmetric quantum well and agrees with numerical calculations for different amounts of surface band bending as shown in Supporting Information Figure S2. It is also fully consistent with quantum oscillation measurements in STO 2DEGs that observed multiple subbands down to very low carrier densities and a splitting of the two lowest lying subbands that increases from  $\approx 1$  to  $\approx 60$  meV when the density increases from  $0.7 \times 10^{13} \text{ cm}^{-2}$  to  $8.7 \times 10^{13} \text{ cm}^{-2}$ .<sup>[7,21]</sup>

In summary, we have shown that it is possible to create and fully deplete the 2DEG found at the (001) surface of STO by alternate in-situ exposure to light and small O<sub>2</sub> doses demonstrating that oxygen vacancies are responsible for its appearance. We explain the photon stimulated O desorption process based on the Ti 3*p* core hole Auger decay which is active at photon energies above  $\sim 38$  eV. In exploiting this knowledge we achieve a new level of control of the OV density on the surface of STO, which allows us to establish the evolution of the subband bandwidth as a function of carrier density in the 2DEG. The observed variations provide strong support for an interpretation of the 2DEG electronic structure in terms of quantum confinement.

## Experimental Section



Experimental Details: La–SrTiO<sub>3</sub> substrates with 0.075wt% La from Crystal Base were fractured *in-situ at temperatures < 30 K*. ARPES measurements were performed at the I05 beamline of the Diamond Light Source and the SIS beamline of the Swiss Light Source. Photon energies between 28 and 140 eV were used with *s*-, *p*- and circularly polarized light. XPS measurements were performed at the I05 beamline of the Diamond Light Source at a photon energy of 650 eV with *p*-polarized light. Samples were measured at temperatures between 6 and 20 K. Results were reproduced on multiple samples.

### Acknowledgements

We gratefully acknowledge discussions with, Milan Radovic, Nick Plumb, Alex Fête and Thomas Greber. This work was supported by the Swiss National Science Foundation (200021-146995). P. D. C. K was supported by the UK-EPSC (EP/I031014/1) and the Royal Society. M. S. B was supported by Grant-in-Aid for Scientific Research from the Ministry of Education, Culture, Sports, Science and Technology of Japan.

- [1] A. Ohtomo, H. Y. Hwang, *Nature* **2004**, *427*, 423.
- [2] N. Reyren, S. Thiel, A. D. Caviglia, L. F. Kourkoutis, G. Hammerl, C. Richter, C. W. Schneider, T. Kopp, A.-S. Rüetschi, D. Jaccard, M. Gabay, D. A. Muller, J.-M. Triscone, J. Mannhart, *Science* **2007**, *317*, 1196.
- [3] A. D. Caviglia, S. Gariglio, N. Reyren, D. Jaccard, T. Schneider, M. Gabay, S. Thiel, G. Hammerl, J. Mannhart, J.-M. Triscone, *Nature* **2008**, *456*, 624.
- [4] M. Ben Shalom, M. Sachs, D. Rakhmievitch, A. Palevski, Y. Dagan, *Phys. Rev. Lett.* **2010**, *104*, 126802.
- [5] C. Richter, H. Boschker, W. Dietsche, E. Fillis-Tsirakis, R. Jany, F. Loder, L. F. Kourkoutis, D. A. Muller, J. R. Kirtley, C. W. Schneider, J. Mannhart, *Nature* **2013**, *502*, 528.
- [6] Y. Z. Chen, N. Bovet, F. Trier, D. V. Christensen, F. M. Qu, N. H. Andersen, T. Kasama, W. Zhang, R. Giraud, J. Dufouleur, T. S. Jespersen, J. R. Sun, A. Smith, J. Nygård, L. Lu, B. Büchner, B. G. Shen, S. Linderoth, N. Pryds, *Nat. Commun.* **2013**, *4*, 1371.
- [7] P. Moetakef, D. G. Ouellette, J. R. Williams, S. James Allen, L. Balents, D. Goldhaber-Gordon, S. Stemmer, *Appl. Phys. Lett.* **2012**, *101*, 1.
- [8] G. Herranz, F. Sánchez, N. Dix, M. Scigaj, J. Fontcuberta, *Sci. Rep.* **2012**, *2*, 758.
- [9] Z. Q. Liu, C. J. Li, W. M. Lü, X. H. Huang, Z. Huang, S. W. Zeng, X. P. Qiu, L. S. Huang, A. Annadi, J. S. Chen, J. M. D. Coey, T. Venkatesan, Ariando, *Phys. Rev. X* **2013**, *3*, 021010.

- [10] K. Ueno, S. Nakamura, H. Shimotani, A. Ohtomo, N. Kimura, T. Nojima, H. Aoki, Y. Iwasa, M. Kawasaki, *Nat. Mater.* **2008**, *7*, 855.
- [11] W. Meevasana, P. D. C. King, R. H. He, S. Mo, M. Hashimoto, A. Tamai, P. Songsiriritthigul, F. Baumberger, Z. Shen, *Nat. Mater.* **2011**, *10*, 114.
- [12] S. McKeown Walker, A. de la Torre, F. Y. Bruno, A. Tamai, T. K. Kim, M. Hoesch, M. Shi, M. S. Bahramy, P. D. C. King, F. Baumberger, *Phys. Rev. Lett.* **2014**, *113*, 177601.
- [13] Z. Wang, Z. Zhong, X. Hao, S. Gerhold, B. Stöger, M. Schmid, J. Sánchez-Barriga, A. Varykhalov, C. Franchini, K. Held, U. Diebold, *Proc. Natl. Acad. Sci. U. S. A.* **2014**, *111*, 3933.
- [14] A. Fête, C. Cancellieri, D. Li, D. Stornaiuolo, A. D. Caviglia, S. Gariglio, J.-M. Triscone, *Appl. Phys. Lett.* **2015**, *106*, 051604.
- [15] Y. Lee, C. Clement, J. Hellerstedt, J. Kinney, L. Kinnischtzke, X. Leng, S. Snyder, a. Goldman, *Phys. Rev. Lett.* **2011**, *106*, 136809.
- [16] A. Joshua, S. Pecker, J. Ruhman, E. Altman, S. Ilani, *Nat. Commun.* **2012**, *3*, 1129.
- [17] M. Stengel, *Phys. Rev. Lett.* **2011**, *106*, 1.
- [18] M. Salluzzo, J. Cezar, N. Brookes, V. Bisogni, G. De Luca, C. Richter, S. Thiel, J. Mannhart, M. Huijben, a. Brinkman, G. Rijnders, G. Ghiringhelli, *Phys. Rev. Lett.* **2009**, *102*, 1.
- [19] A. D. Caviglia, S. Gariglio, C. Cancellieri, B. Sacépé, A. Fête, N. Reyren, M. Gabay, A. F. Morpurgo, J. M. Triscone, *Phys. Rev. Lett.* **2010**, *105*, 236802.
- [20] A. Fête, S. Gariglio, A. D. Caviglia, J. M. Triscone, M. Gabay, *Phys. Rev. B.* **2012**, *86*, 1.
- [21] A. McCollam, S. Wenderich, M. K. Kruize, V. K. Guduru, H. J. A. Molegraaf, M. Huijben, G. Koster, D. H. A. Blank, G. Rijnders, A. Brinkman, H. Hilgenkamp, U. Zeitler, J. C. Maan, *APL Mater.* **2014**, *2*, DOI 10.1063/1.4863786.
- [22] G. Berner, M. Sing, H. Fujiwara, A. Yasui, Y. Saitoh, A. Yamasaki, Y. Nishitani, A. Sekiyama, N. Pavlenko, T. Kopp, C. Richter, J. Mannhart, S. Suga, R. Claessen, *Phys. Rev. Lett.* **2013**, *110*, 247601.
- [23] C. Cancellieri, M. L. Reinle-Schmitt, M. Kobayashi, V. N. Strocov, P. R. Willmott, D. Fontaine, P. Ghosez, A. Filippetti, P. Delugas, V. Fiorentini, *Phys. Rev. B* **2014**, *89*, 121412.
- [24] A. F. Santander-Syro, O. Copie, T. Kondo, F. Fortuna, S. Pailhès, R. Weht, X. G. Qiu, F. Bertran, A. Nicolaou, A. Taleb-Ibrahimi, P. Le Fèvre, G. Herranz, M. Bibes, N. Reyren, Y. Apertet, P. Lecoeur, A. Barthélémy, M. J. Rozenberg, *Nature* **2011**, *469*, 189.
- [25] P. D. C. King, S. McKeown Walker, A. Tamai, A. de la Torre, T. Eknapakul, P. Buaphet, S.-K. Mo, W. Meevasana, M. S. Bahramy, F. Baumberger, *Nat. Commun.* **2014**, *5*, 3414.

- [26] H. O. Jeschke, J. Shen, R. Valenti, *New J. Phys.* **2014**, *17*, 6.
- [27] C. Lin, A. A. Demkov, *Phys. Rev. Lett.* **2013**, *111*, 217601.
- [28] F. Lechermann, L. Boehnke, D. Grieger, C. Piefke, *Phys. Rev. B* **2014**, *90*, 1.
- [29] M. Sing, G. Berner, K. Goß, A. Müller, A. Ruff, A. Wetscherek, S. Thiel, J. Mannhart, S. a. Pauli, C. W. Schneider, P. R. Willmott, M. Gorgoi, F. Schäfers, R. Claessen, *Phys. Rev. Lett.* **2009**, *102*, 1.
- [30] E. Slooten, Z. Zhong, H. J. A. Molegraaf, P. D. Eerkes, S. de Jong, F. Massee, E. van Heumen, M. K. Kruize, S. Wenderich, J. E. Kleibeuker, M. Gorgoi, H. Hilgenkamp, A. Brinkman, M. Huijben, G. Rijnders, D. H. A. Blank, G. Koster, P. J. Kelly, M. S. Golden, *Phys. Rev. B* **2013**, *87*, 085128.
- [31] F. Lechermann, L. Boehnke, D. Grieger, C. Piefke, *Phys. Rev. B* **2014**, *90*, 085125.
- [32] M. Knotek, P. Feibelman, *Phys. Rev. Lett.* **1978**, *40*, 964.
- [33] M. L. Knotek, *Phys. Today* **1984**, *37*, 24.
- [34] O. Dulub, M. Batzilln, S. Solovev, E. Loginova, A. Alchagirov, T. E. Madey, U. Diebold, *Science* **2007**, *317*, 1052.
- [35] S. Moser, L. Moreschini, J. Jaćimović, O. S. Barišić, H. Berger, A. Magrez, Y. J. Chang, K. S. Kim, A. Bostwick, E. Rotenberg, L. Forró, M. Grioni, *Phys. Rev. Lett.* **2013**, *110*, 196403.
- [36] A. F. Santander-Syro, F. Fortuna, C. Bareille, T. C. Rödel, G. Landolt, N. C. Plumb, J. H. Dil, M. Radović, *Nat. Mater.* **2014**, *13*, 1085.

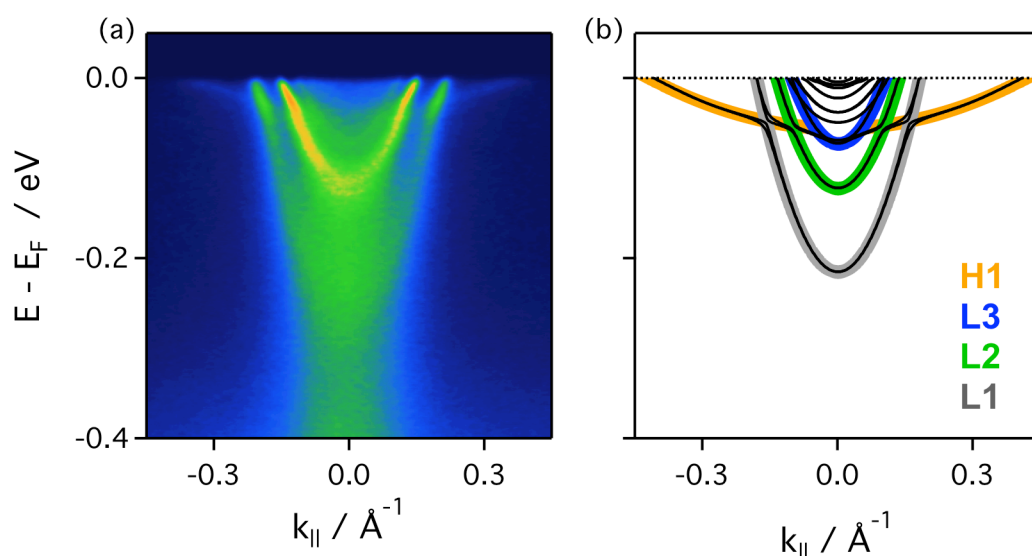


**Figure 1. Electronic structure of the 2D electron gas in SrTiO<sub>3</sub>(001).** (a) Energy momentum dispersion plot measured in the second Brillouin zone. Measurements shown are the sum of data taken with s- and p- polarized light at 52 eV photon energy and T = 10 K. (b) Tight binding supercell calculations (black). The three light bands (L1, L2, L3) and the heavy band (H1) resolved in the ARPES measurement are marked in grey, green, blue and orange respectively. L1, L2 and L3 have predominantly xy-orbital character and H1 has predominantly xz/yz-orbital character.

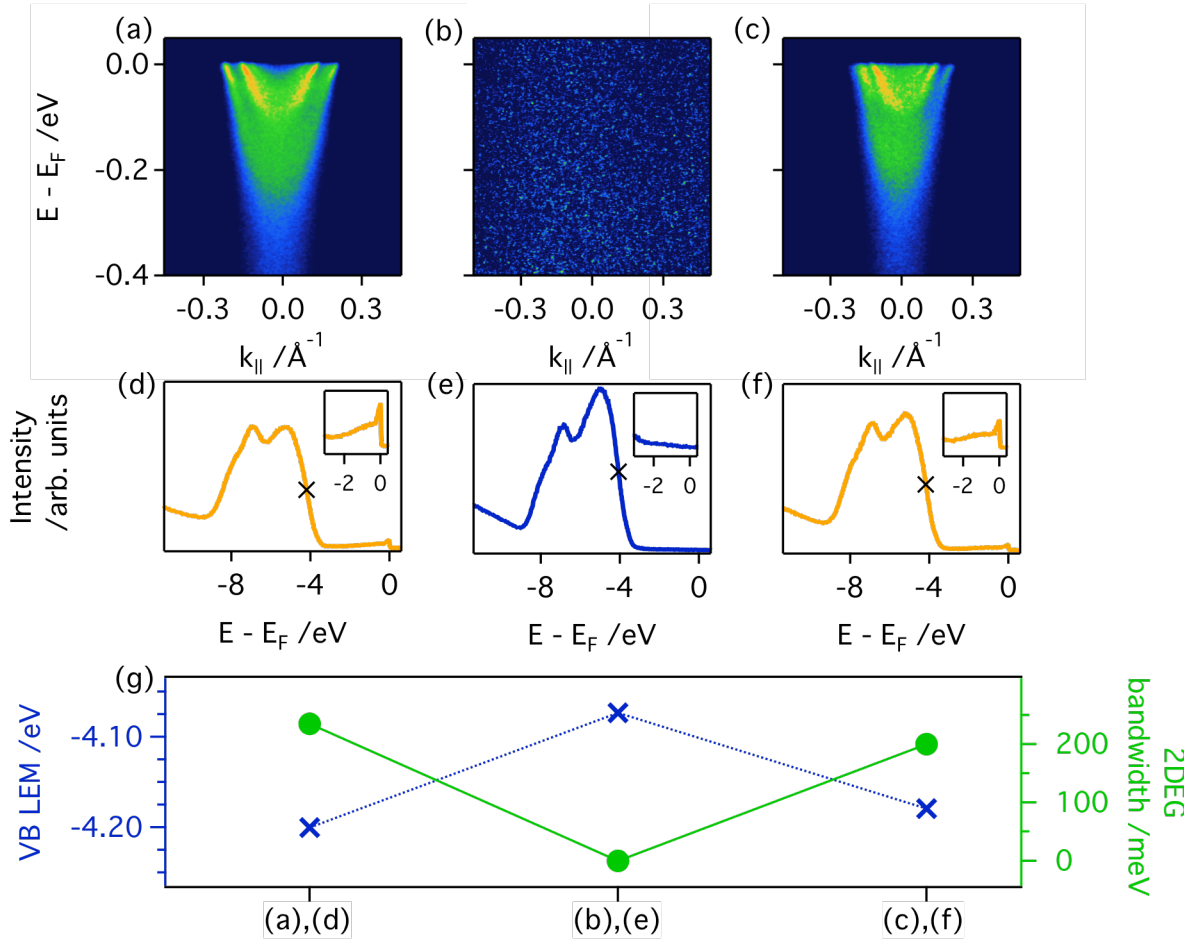


**Figure 2. The effect of oxygen on the 2DEG and valence band of the STO(001) surface.** (a) Dispersion plot of the high density STO(001) surface 2DEG after initial irradiation with 52 eV photons. (b,c) The 2DEG disappears after *in-situ* exposure to 0.5 Langmuir of  $O_2$  and reappears following further irradiation with 52 eV photons. (d-f) Angle integrated valence band spectra corresponding to the states in (a-c). The magnified insets show the intensity at the Fermi level. The valence band leading edge midpoint (VB LEM) is marked by a cross. (g) VB LEM and 2DEG bandwidth that correspond to the states shown in (a-c) and (d-f). All data were measured in the second Brillouin zone with 28 eV, s-polarized light.

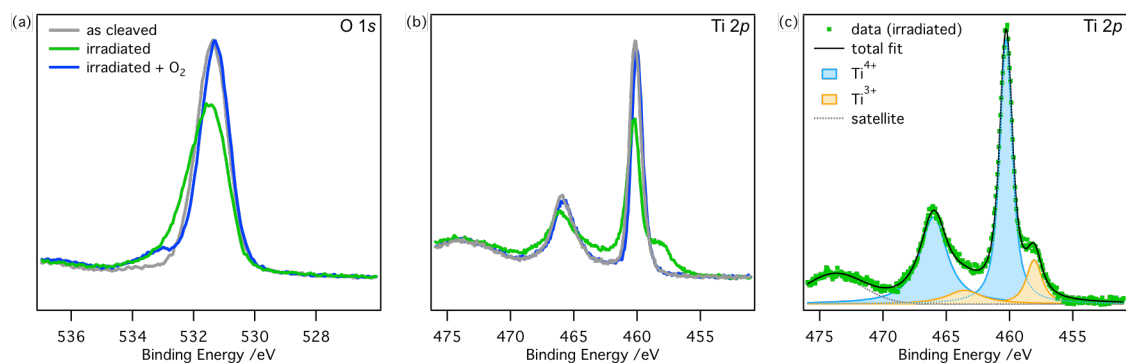


**Figure 3. Core level spectroscopy.** (a,b) X-ray photoemission spectra of Oxygen 1s and Titanium 2p core levels on the (grey) as-cleaved, (green) irradiated and (blue) oxygen exposed (0.4 Langmuir) STO(001) surface. The spectra are normalized to the background on the low binding energy side of the peaks. (c) Fit to the spin orbit split Ti2p<sub>1/2</sub> and Ti2p<sub>3/2</sub> peaks of the irradiated surface. The Ti 3+ and 4+ peaks are shown in orange and blue shading respectively.

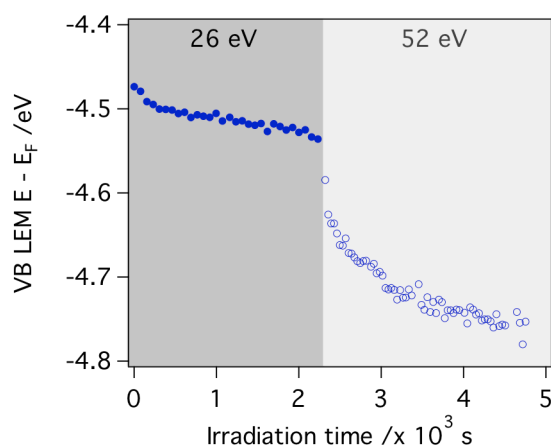


**Figure 4. Evidence for oxygen vacancy creation by core hole Auger decay.** Valence band leading edge mid-point as a function of irradiation time at  $h\nu = 26$  eV (solid symbols) and 52 eV (open symbols). All points were measured consecutively at the same sample position.

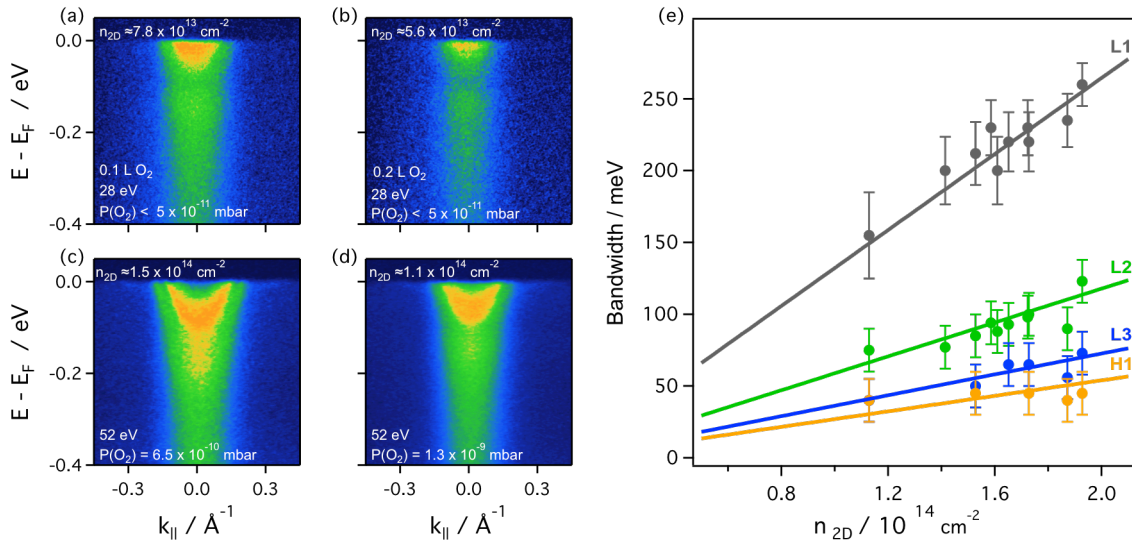


**Figure 5. Control of the STO(001) surface 2DEG density.** (a,b) Dispersion plot measured with 28 eV photons on a surface that initially supported a saturated 2DEG and was subsequently exposed to 0.1 and 0.2 Langmuir  $\text{O}_2$ . (c,d) Dispersion plots measured with 52 eV photons in an oxygen partial pressure of  $5 \times 10^{-10}$  mbar and  $2 \times 10^{-9}$  mbar, respectively. (e) Occupied bandwidth as a function of carrier density for the first three light subbands (L1, L2, L3) and the first heavy subband (H1) indicated in grey, green, blue and orange respectively.